Archives of Biochemistry and Biophysics 714 (2021) 109066

Contents lists available at ScienceDirect

Archives of Biochemistry and Biophysics

journal homepage: www.elsevier.com/locate/yabbi

Mammalian dihydropyrimidine dehydrogenase

Dariush C. Forouzesh, Graham R. Moran *

Department of Chemistry and Biochemistry, 1068 W Sheridan Rd, Loyola University Chicago, Chicago, IL, 60660, USA

ARTICLE INFO

Keywords:
Flavin
Iron-sulfur
Hydride
Oxidoreductase
Dehydrogenase
Pyrimidine

ABSTRACT

Dihydropyrimidine dehydrogenase (DPD) catalyzes the two-electron reduction of pyrimidine bases uracil and thymine as the first step in pyrimidine catabolism. The enzyme achieves this simple chemistry using a complex cofactor set including two flavins and four Fe_4S_4 centers. The flavins, FAD and FMN, interact with respective NADPH and pyrimidine substrates and the iron-sulfur centers form an electron transfer wire that links the two active sites that are separated by 56 Å. DPD accepts the common antineoplastic agent 5-fluorouracil as a substrate and so undermines the establishment of efficacious toxicity. Though studied for multiple decades, a precise description of the behavior of the enzyme had remained elusive. It was recently shown that the active form of DPD has the cofactor set of FAD-4(Fe_4S_4)-$FMNH_2$. This two-electron reduced state is consistent with fewer mechanistic possibilities and data suggests that the instigating and rate determining step in the catalytic cycle is reduction of the pyrimidine substrate that is followed by relatively rapid oxidation of NADPH at the FAD that, via the electron conduit of the 4(Fe_4S_4) centers, reinstates the $FMNH_2$ cofactor for subsequent catalytic turnover.

1. Introduction

Dihydropyrimidine dehydrogenase (DPD) catalyzes the first step of pyrimidine catabolism by promoting the reduction of the 5,6-vinylic bond of thymine or uracil with electrons acquired from NADPH (Scheme 1).

DPD has considerable clinical significance as it accepts the pervasive chemotherapeutic 5-fluorouracil as a substrate, severely shortening its pharmacological half-life and dictating the use of elaborate compensatory administration protocols to achieve efficacious toxicity [1,2]. The pyrimidine reduction reaction catalyzed by DPD is similar to the reaction catalyzed by dihydroorotate dehydrogenase (DHOD), an enzyme that oxidizes the 5,6-bond of dihydroorotate to orotate as part of pyrimidine biosynthesis. Despite the simple net hydride transfer chemistry, DPD uses an elaborate cofactor set to facilitate pyrimidine reduction. Mammalian DPD is a functional homodimer and each subunit contains an FAD, an FMN and four Fe_4S_4 centers with two Fe_4S_4 centers from each subunit forming an electron transfer conduit that link the flavins within each subunit. The catalysis of DPD has been studied for five decades, but its unconventional architecture and catalytic behavior has largely impeded detailed assessment of its catalytic mechanism. Recent observations have revealed unexpected sequences of redox cycling and hydrogen transfers that have narrowed the mechanistic possibilities. The purpose of this review is to describe these advances in the context of prior mechanistic and clinical observations that have been reported for this enzyme.

2. Clinical significance

5-Fluorouracil (5FU) and 5FU prodrugs are among the most-commonly prescribed cytotoxic agents used in the treatment of cancer. In the United States approximately 570,000 courses of treatment are prescribed each year. 5FU was synthesized and offered as a potential inhibitor of tumor cells when it was discovered that liver tumor cells sequestered uracil at a rate above that of normal liver cells [3,4]. 5FU has since proven to be one of the more versatile and durable cancer therapeutics and remains as the central component of the standard of care for colorectal, specific types of breast, aerodigestive, ovarian, head and neck, and skin cancers. With near equivalent shape to that of uracil, 5FU is incorporated into RNA and DNA via the nucleotide 5FUMP (Fig. 1).

RNA and DNA biosynthesis are linked via the activity of ribonucleotide reductase (RR) that will convert 5FUDP to 5FdUDP, which when dephosphorylated to form 5FdUMP becomes a potent inhibitor of thymidylate synthase (TS) [5]. 5FU is therefore able to stall *de novo* synthesis of thymine nucleotides, halting cell division and inducing

Abbreviations: DPD, Dihydropyrimidine dehydrogenase; DHOD, dihydroorotate dehydrogenase; 5FU, 5-fluorouracil; 5EU, 5-ethynyluracil; 5IU, 5-iodouracil.

* Corresponding author.
E-mail address: gmoran3@luc.edu (G.R. Moran).

https://doi.org/10.1016/j.abb.2021.109066
Received 14 September 2021; Received in revised form 21 October 2021; Accepted 23 October 2021
Available online 27 October 2021

apoptosis [6,7]. While toxic to all cells, 5FU is particularly toxic to cells undergoing rapid growth and division. However, 5FU is rapidly detoxified ($t_{1/2}$~8–14 min) by DPD [1,5,8–13]. The efficiency with which DPD detoxifies 5FU has meant that patients are typically administered a bolus followed by ~48 h of continuous infusion using an ambulatory pump coupled to a central venous catheter. Infusion via the pump can provide sustained 5FU levels but incurs complications of infection, thrombosis and reduced compliance. Moreover, the 30-fold variability of net DPD activity in individual patients means that dosing for optimal tolerance and efficacy is difficult [1,2,14–18]. Inhibition of DPD activity has been extensively offered as the means to reliably attain and sustain patient specific optimal dosing [9,19–21]. 5FU can also be administered orally as the prodrug, capecitabine, but as a consequence of DPD activity the cellular 5FU concentrations achieved are dramatically lower than by infusion [22]. Inhibition of DPD would therefore also potentially provide a path to an improved therapeutic index for capecitabine-based 5FU administration [23,24] that would in turn increase both compliance and neoplastic toxicity while also reducing infection rates and cardio-thrombic complications associated with indwelling central venous catheters. Inhibition of DPD has consequently been a prominent component of research of the enzyme. Inhibitors of DPD have universally been pyrimidine analogs with modifications to the substituent at the C5 of the pyrimidine ring. Two such molecules are 5-ethynyluracil (5EU) and 5-iodouracil (5IU) (Scheme 2). 5EU inhibits DPD by thiol-yne click chemistry with the thiol of the pyrimidine active site general acid cysteine [25,26] (see below) irreversibly inactivating the enzyme.

5IU also has been shown to inhibit DPD through covalent modification of the same residue, but has not been studied extensively. It is thought that 5IU is a substrate for DPD and the product, 5-iodo-5,6-dihydrouracil, is the inhibiting form of the ligand that induces nucleophilic attack by the active site cysteine acid with displacement of the iodo-group [27]. Mechanistic aspects of DPD inhibition by 5EU will be discussed below in the context of structural changes that occur during catalysis.

3. Structure of DPD

Dobritzsch et al. were first to report X-ray crystal structures of porcine DPD and so can be credited with much of our current structural understanding of the enzyme [28,29]. Consequently, throughout this review residue numbering will reference the primary structure of the porcine enzyme. The initial structural analyses were later comprehensively compiled in a review article by Schnackerz et al. [30] and will be summarized briefly here. Each 1025 amino acid subunit of DPD has five domains (Fig. 2). Domain I (residues 27–173) is comprised solely of α-helices and contains two Fe_4S_4 centers near the N-terminus that are proximal to the FAD and NADPH binding site. The Fe_4S_4 center most proximal to the FAD has a unique ligand arrangement with three cysteines and one glutamine coordinating the iron ions of the cluster [31]. Domain II (residues 174–286, 442–524) consists of a parallel β-sheet stacked with α-helices and houses the FAD binding site. Domain III (residues 287–441) consists of antiparallel and parallel β-sheet, the latter of which is stacked with α-helices to form the NADPH substrate binding site.

The combined topology of domains II and III are highly similar to adrenodoxin reductase [32,33] and when added to domain I form a structural module whose topology can be identified in other multi-flavin-dependent enzymes that each use intervening iron-sulfur clusters to deliver electrons between flavins (Fig. 3) [34].

Domain IV (residues 525–847) is an $\alpha_8\beta_8$ TIM barrel fold [35] that forms the binding site for the FMN cofactor and substrate pyrimidines that are localized ~60 Å distant from the NADPH active site formed by domains II and III. A catalytically critical residue, C671, resides in Domain IV proximal to the pyrimidine binding site. This residue has been shown to donate its sulfhydryl proton to complete pyrimidine reduction [26,28,30,36–39]. Domain V (residues 1–26, 848–1025) contains the two C-terminal Fe_4S_4 centers that lie adjacent to the pyrimidine active site of the partner subunit.

Domain IV resembles the structure of *Lactococcus lactis* class 1A dihydroorotate dehydrogenase (DHOD), an enzyme that catalyzes a similar reaction oxidizing 5,6-dihydroorotate to orotate as the fourth step of *de novo* pyrimidine biosynthesis [40,41]. Domain IV also resembles the N-terminal domain of the class 1B DHODs establishing that the machinery for redox chemistry in the catabolism and synthesis of pyrimidine bases is largely conserved (Fig. 2). Furthermore, class 1B DHODs have FAD and FMN cofactors each bound at separate sites that are bridged by a single Fe_2S_2 center. These sites interact with $NADP^+$ and 5,6-dihydroorotate respectively, and so the cofactors are arranged similarly to those observed in DPD [42].

All five domains have contact with the adjacent subunit and collectively form a subunit-subunit interface of ~10,800 $Å^2$ [28]. DPD has been shown to be rigid in its tertiary and quaternary structures. When comparing the structures of holoenzyme and ternary complex of wild type DPD, the only significant deviation in the structure is the conformation of the 669–684 loop, an apparently mobile protein segment that contains the general acid residue, C671. The ligand-free DPD as well as pyrimidine binary complexes were shown to have the mobile loop in an open position with C671 positioned ~10 Å from the site occupied by the C5 of the pyrimidine. The closed form of DPD is observed only in the NADP(H) and pyrimidine ternary complex. In this position C671 is ~3.3 Å from the pyrimidine C5, a position clearly more conducive to proton transfer [26,28,29].

The DPD architecture suggests that the FAD, FMN, NADPH, pyrimidines and two Fe_4S_4 centers from each subunit form a linear electron conduit that shunts electrons from NADPH to pyrimidine substrates (Fig. 4). Two Fe_4S_4 centers and the FAD cofactor are coordinated by domain I and II of the same subunit. The Fe_4S_4 centers nearest the FMN cofactor are from the domain V of the adjacent subunit. As such electrons traverse a path that includes parts of both subunits of the DPD

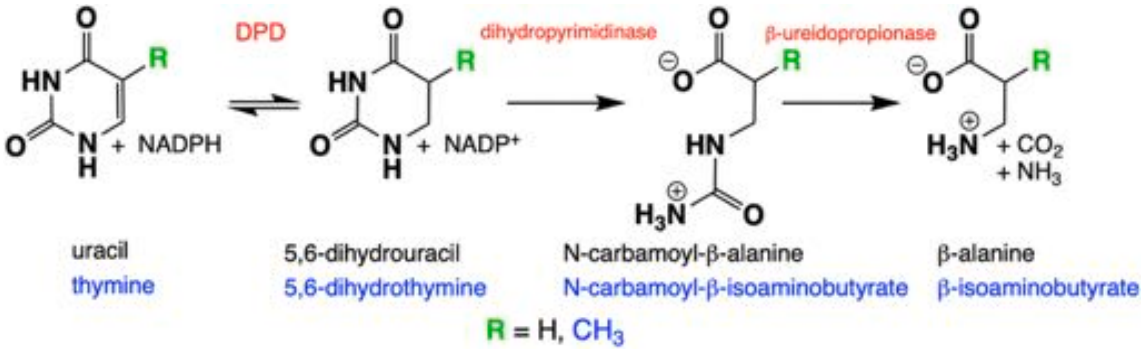

Scheme 1. Pyrimidine Catabolism.

dimer. This ~60 Å transmission of electrons is formally only inferred from the structure as no observation has yet recorded a reduced state of the Fe_4S_4 centers during catalysis [26,36,37,39,43]. The available structures however do plainly imply that catalysis begins with transfer of a hydride from NADPH to the isoalloxazine of FAD and that these electrons then transmit through the Fe_4S_4 centers to the FMN and on to the pyrimidine.

It can be assumed that electrons travel sequentially through the obligate one-electron acceptor/donor Fe_4S_4 centers [31]. It is therefore expected that the flavins will cycle between oxidized, hydroquinone and semiquinone states during catalysis to receive and transmit electrons through the chain of Fe_4S_4 centers. A hydride equivalent is transferred to the FMN and then to the C6 of the pyrimidine and this is reliant on proton addition from the thiol of C671 to the pyrimidine C5 [30,44]. The precise sequence of events that bring about pyrimidine reduction are not known, though recent advances have confined the mechanistic possibilities considerably (see below).

4. The interactions of substrates within the active sites

In Figs. 5 and 6 the ligand interactions of NADPH and pyrimidine are depicted. In Fig. 5 NADPH is observed to bind with its dihydronicotinamide ring localized conventionally with respect to the FAD [45]. The nicotinamide ring is stacked parallel to the FAD isoalloxazine with its C4 2.9 Å from the flavin N5 (gap depicted in orange). DPD has non-covalent interactions primarily with the AMP nucleotide of NADPH where a clustering of positively charged residues form ion pairing interactions with the 3′-phospho-group of the AMP ribose and the pyrophosphate moiety. Single hydrogen bonding interactions are also observed for the adenine and ribose moieties of AMP. Curiously, no hydrogen bonds are observed for the nicotinamide riboside. This single charge pairing interaction for the pyrophosphate added to five negative and one positively charged residue near the stacked dihydronicotinamide•isoalloxazine complex may function to lower the reduction potential of the FAD and thereby facilitate electron transfer to the iron sulfur center conduit.

Fig. 6 shows the FMN/pyrimidine active site ligand interactions and the observed conformational states of the 669–684 loop. Pyrimidine substrates are localized adjacent and parallel to the FMN isoalloxazine by six apparent hydrogen bonding interactions; five of which are from the amide residues, N609, N668 and N736 and one from T737. This binding pose places the pyrimidine C6 3.6 Å from the N5 of the FMN isoalloxazine, a position favorable for hydride transfer. The movement of the 669–684 loop toggles the position of the active site acid, C671 by 7.7 Å such that in the *in* position (depicted in green) the thiol sulfur is 3.3 Å from the C5 of the pyrimidine (distance shown in orange). There are no interactions within 4 Å of the pyrimidine C5 position, consistent with the acceptance of uracil, thymine and other 5-substituted uracils as substrates [1,27,46]. Two lysine residues first recognized by Dobritzsch et al., K574 and K709, are within hydrogen bond distance to the FMN N5 and N1 of the isoalloxazine respectively [28]. The function of these residues has not been investigated, however there exists requirements to accept (N5) and donate (N1) protons as the FMN is reduced in successive one-electron steps and then oxidized with hydride transfer. These lysine residues are oriented to participate in such acid/base chemistry. Furthermore, the positive potential of these basic residues may raise the redox potential of the FMN such that it can act as the electron sink in the conduit of electron transfer from NADPH.

5. Mechanistic studies of DPD

The steps of pyrimidine catabolism were mapped throughout the 1950's and onward [47,48] and the record of enzymatic research of DPD commences around 1970 [49]. The majority of early studies describe purification from endogenous sources and basic steady-state analyses [46,50–54]. This advanced through the 1990s and 2000s to pre-steady state kinetics, kinetic isotope effects, spectroscopic studies and investigations of the wild type relative to variant forms of DPD [36,37,43,

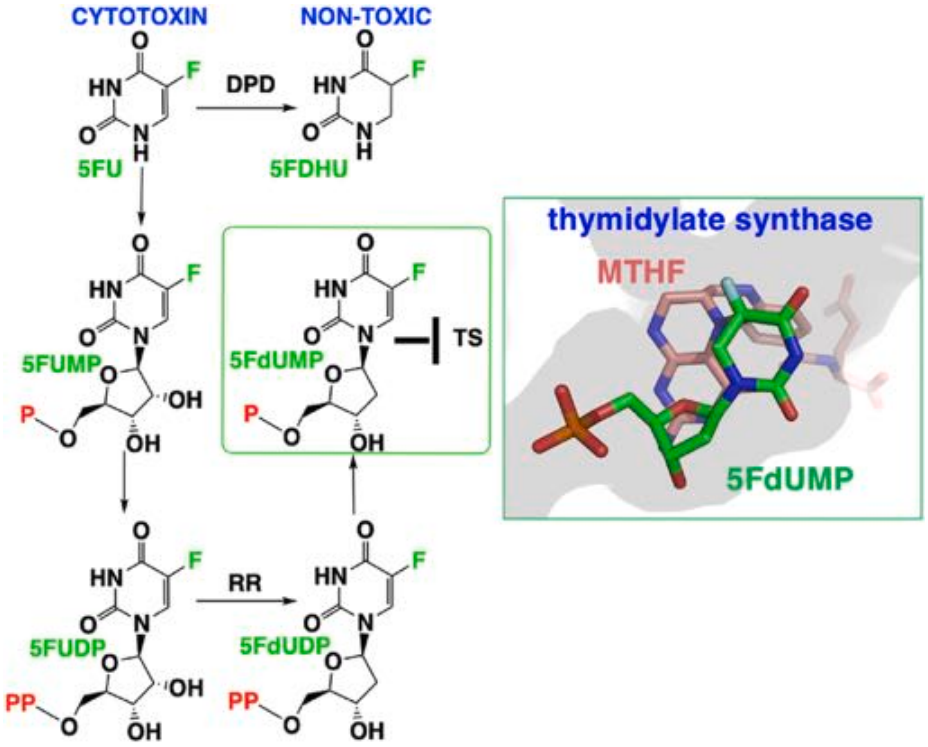

Fig. 1. Metabolism of 5- Fluorouracil. 5FU is initially incorporated into RNA nucleotides. Ribonucleotide reductase (RR) accepts 5FUDP as a substrate leading to the production of 5FdUMP. 5FdUMP forms an inhibitory ternary complex with methylenetetrahydrofolate (MTHF) and thymidylate synthase (TS), limiting the production of thymidylate.

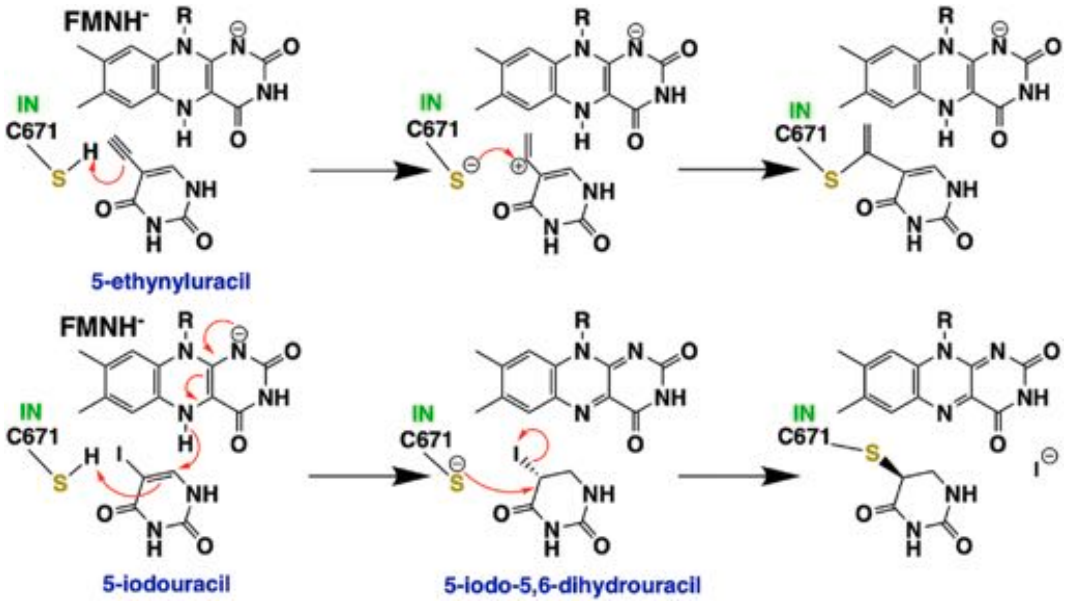

Scheme 2. Proposed Mechanisms for Inactivation of DPD by 5-Ethynyluracil and 5-Iodouracil.

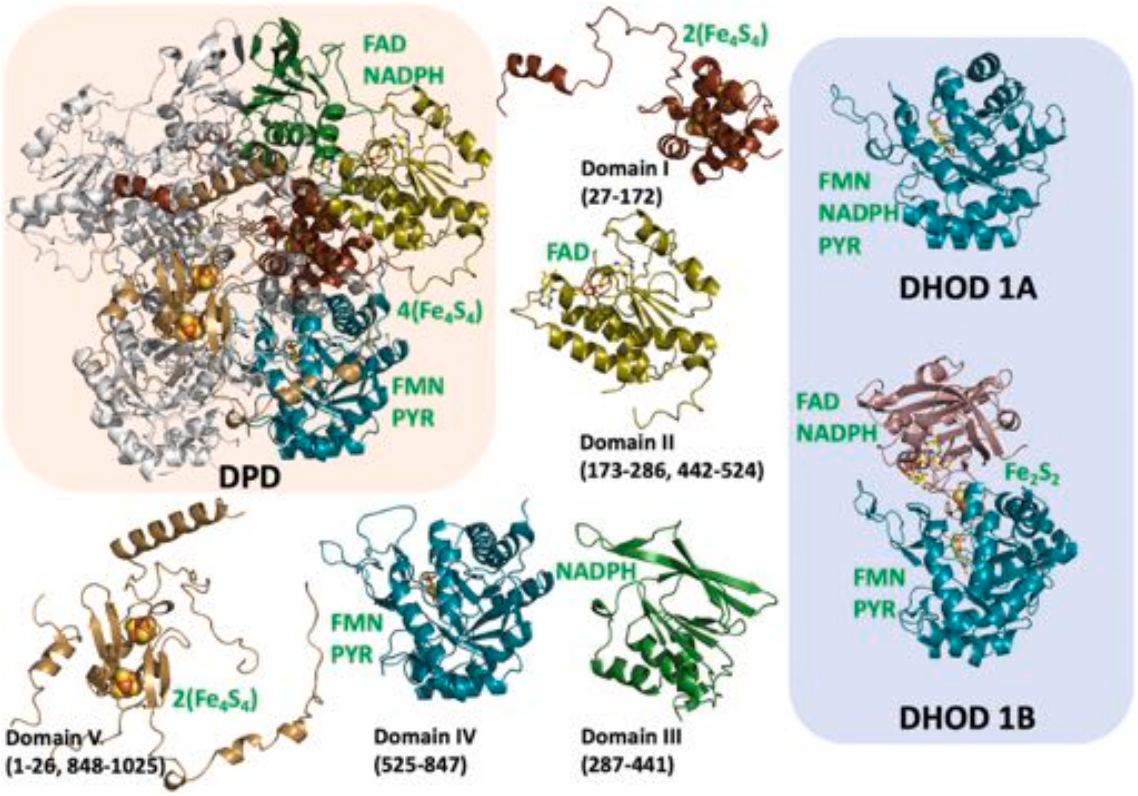

Fig. 2. The domains of DPD.

44]. As stated, the first structures of DPD were reported in the early 2000s [28,29,55] and given its unexpected and elaborate cofactor set, it is fair to surmise that the lack of structural data during the prior three decades confounded efforts to comprehend how the enzyme functions [36,43]. Evidence for this is apparent in the chronology of reports for cofactor content. DPD has been purified from human, murine, ovine, and porcine tissues [46,50,56,57] and the porcine enzyme has been expressed heterologously in *E. coli* [36,58] and the analytical accounts for cofactor content for these preparations vary considerably.

Despite the lack of structural data for DPD, collaborative studies between the Cook and Schnackerz laboratories developed much of the foundational mechanistic understanding of the enzyme [30,50,51,53]. In particular, the notion of physically separate enzymatic half-reactions was established by these authors. In 1990 Podschun et al. published a study of the steady-state kinetic mechanism of DPD [51]. At low concentrations competitive inhibition by NADPH versus uracil was observed and uncompetitive inhibition by uracil for NADPH. Product inhibition and dead-end inhibition using ATP-ribose and 2,

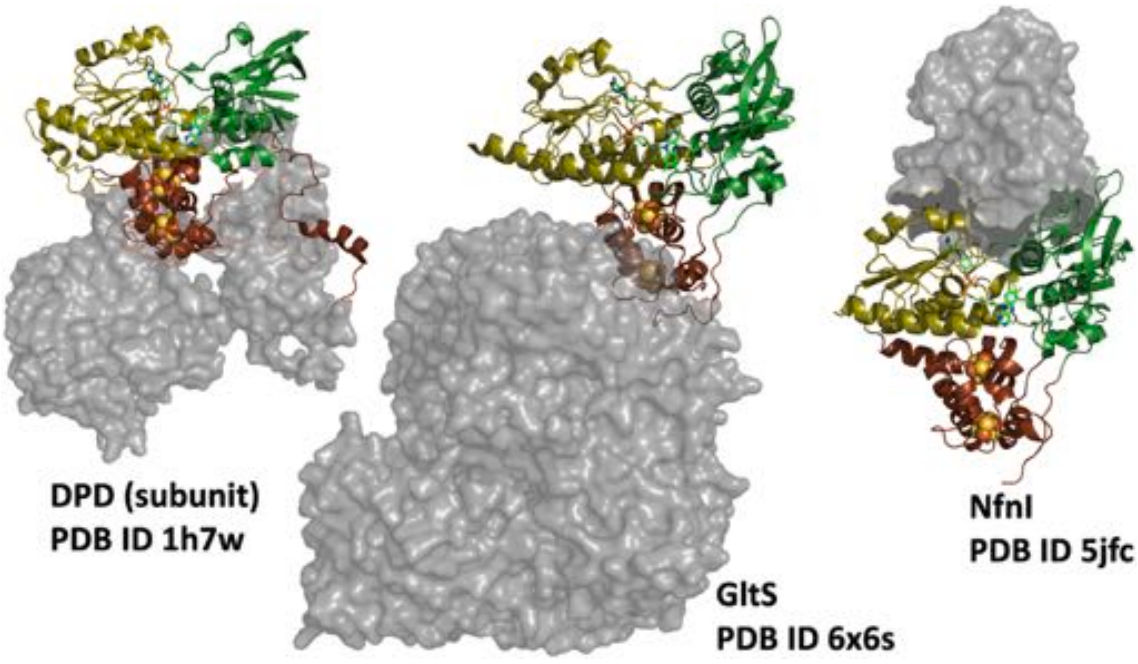

Fig. 3. The conserved electron insertion module. Domains I, II and Ill of DPD comprise $2Fe_4S_4$, FAD and NADPH binding domains and form a conserved structural feature that is also observed in bacterial glutamate synthase (GItS) and NADH-dependent ferredoxin:NADP oxidoreductase (Nfnl).

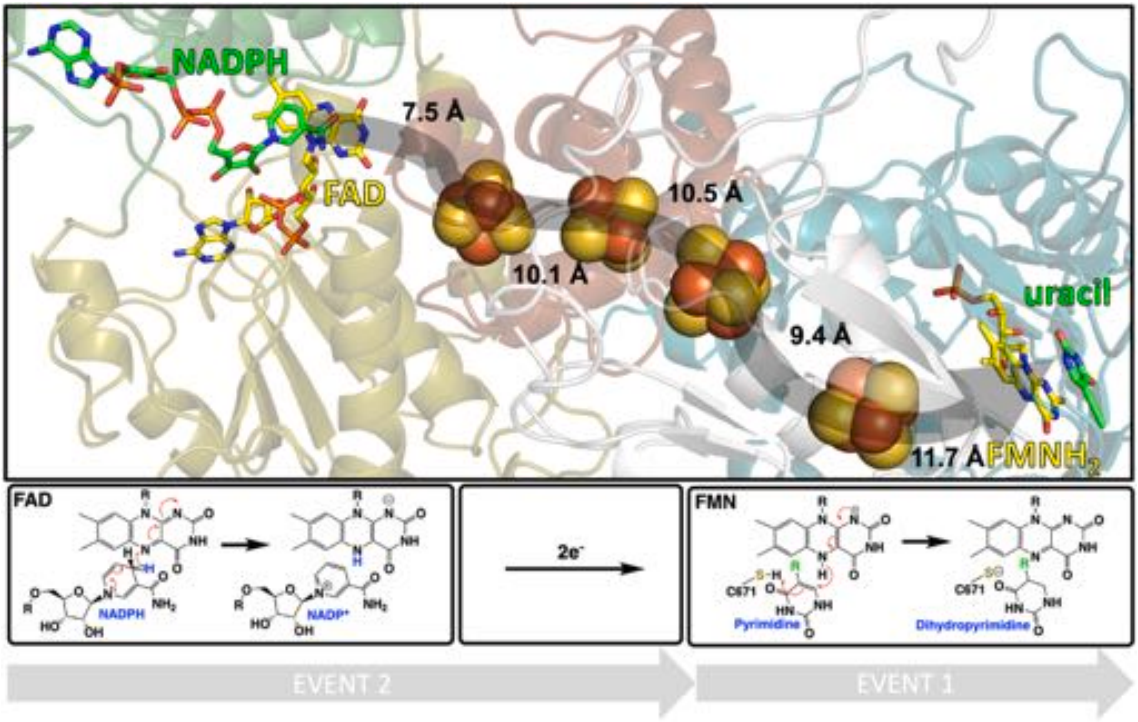

Fig. 4. The Proposed Electron Transfer Path and Reaction Sequence of DPD. Distances indicate the proximities of cofactors.

6-dihydroxypyridine was suggestive of an unconventional two-site ping pong mechanism in which $NADP^+$ dissociation constituted the requisite irreversible step under initial velocity conditions [51].

Three years later Podschun and coworkers published a very detailed pH and solvent kinetic isotope effect study of DPD using steady state approaches [53]. In this study a $^{D}k_{cat}/K_m$NADPH kinetic isotope effect (KIE) of ~1.1 was observed that suggested hydride transfer to FAD is not significantly rate limiting in this half reaction. Solvent kinetic isotope effects (SKIE) for k_{cat}/K_mNADPH of ~2 and for k_{cat} of ~3 were interpreted as derived from the movement of protons at the FAD having significant contribution to the turnover number. From pH dependencies, pKas of 5.8 and 8.2 were observed for k_{cat}/K_mNADPH and were said to be derived from proton movements associated with conformational changes with NADPH binding. Later in a review article published after the first DPD structures were reported, D342 was implicated as the source of the 5.8 value and R235 proposed to be the base abstracting a proton from the FAD N5 with reduction (Fig. 5). These researchers also noted that no groups with dissociable protons were located adjacent to

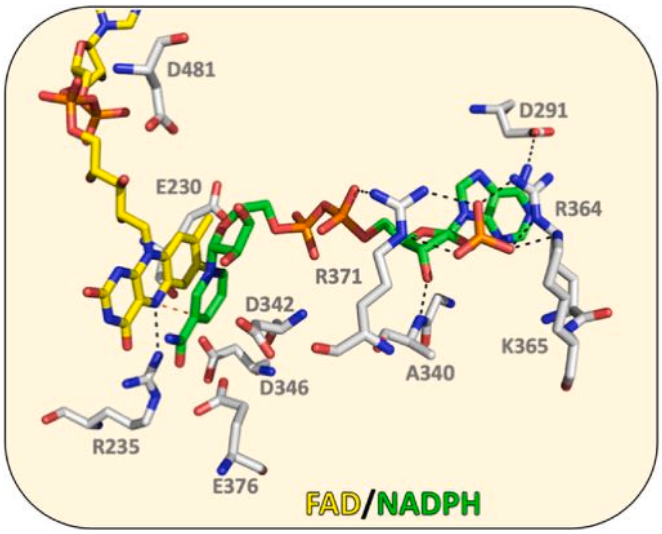

Fig. 5. The FAD/NADPH active site ligand interactions of DPD.

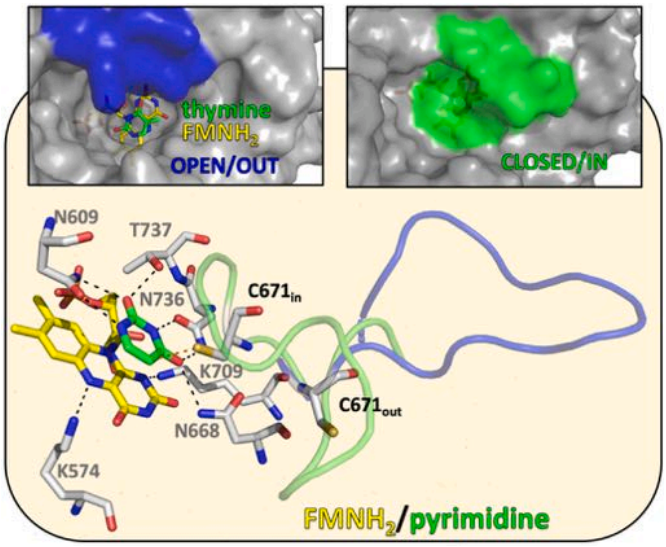

Fig. 6. The $FMNH_2$/Pyrimidine Active Site Ligand Interactions of DPD. A. The complex of NADP(H) with the FAD active site. B. The complex of uracil with the FMN active site. The two positions of the dynamic loop (669–684) are show in green and blue. Insets depict the surface rendering of the acive site cavity proximal to the $FMNH_2$ active site. Left inset has the loop residues 669–684 colored in blue and the right inset has these residues colored green.

N1 of the FAD, suggesting transient formation of the anionic FAD hydroquinone is favored [30].

In the 1993 study by Podschun et al., steady state data that report chemistry at the FMN/pyrimidine active site were SKIEs on k_{cat}/K_mUracil of ~0.7 consistent with ionization of a thiol residue in the events of the half reaction at this site. A SKIE on k_{cat} of ~3.3 is consistent with the transfer of a solvent derived proton in the rate limiting step and was confirmed in later transient state SKIE measured for pyrimidine reduction [39]. pKas of 5.6 and 9.1 observed for k_{cat}/K_mUracil were later proposed to arise from titration of C671 and K709 respectively. As mentioned, the two lysine residues K574 and K709 are proposed to be the general acid/base residues that abstract and supply protons to N5 and N1 respectively during redox cycling of the FMN cofactor (Fig. 6) [30].

Characterization of DPD from bovine liver was conducted using steady state and pre-steady state kinetics [54]. The data obtained suggested the enzyme has a random rapid-equilibrium mechanism with independent dissociation constants for uracil and NADPH. DPD was shown to readily catalyze the exchange of tritium from Pro-S NADPT for solvent protons; this exchange rate was maintained even when using 5EU-inactivated DPD. This supported a separate active site model because, as stated, 5EU covalently links itself near the pyrimidine active site while having no influence on NADPH binding. The first order rate constant of deuterium exchange for bound Pro-S NADPD with solvent protons was 5.4 s^{-1}, more rapid than the reported k_{cat} of 1.6 s^{-1}, further validating the proposed rapid-equilibrium mechanism. These data were similar to those of Podschun et al., 1990 who showed exchange of radio-label between $NADPH/NADP^+$ and uracil/dihydrouracil pairs [51] indicating reversible hydride transfer at both flavins independent of catalytic turnover.

Rosenbaum et al. published secondary tritium isotope effects for 5-^{3}H-uracil in H_2O and D_2O. The only modestly more inverse KIE in deuterium solvent (0.9 vs 0.85) suggested that the hydride transfer and protonation required to reduce pyrimidines were not concerted. These authors argued for a stepwise transfer of the hydride from $FMNH_2$ and a proton from an active site acid. In a separate study published in the same year Rosenbaum et al. reported the first anaerobic transient state data for recombinant porcine DPD. This study measured ligand binding equilibria and included enzyme monitored turnover data that report spectrophotometric changes of the enzyme in the presence of excess substrates [36,59]. This investigation documented a number of observations that interlock with recent findings (see below). Specifically, ligand binding data indicated low micromolar dissociation constants for uracil and NADPH, which create near first-order conditions in transient state experiments at low substrate concentrations. When DPD was mixed with NADPH with or without pyrimidine under anaerobic conditions, multiphasic fractional reduction involving one flavin per dimer without evidence of reduction of the Fe_4S_4 centers was observed. In the absence of pyrimidine, reduction occurred with a rate many-fold slower than catalysis (0.02 s^{-1}). Anaerobic reduction of WT DPD by NADPH alone has also been studied by Podschun et al. who showed that incubation of NADPH with DPD in D_2O brought about the incorporation of deuterium into the Pro-S position of the C4 of NADPH [53]. Later Beaupre et al. observed the kinetics of reduction of DPD by NADPH in the absence of pyrimidines under anaerobic conditions. Titration of NADPH showed a corresponding absorption change at 440 nm with first-order reaction behavior for saturating concentrations. Similar to the observations of Rosenbaum et al., the kinetic traces were fit to two exponentials with rate constants of ~2 and ~0.04 s^{-1}; the latter of which was approximately 10 to 20-fold lower than the steady state turnover number for WT DPD in the presence of uracil and thymine respectively and was therefore assigned as not catalytically relevant [38]. The total extinction coefficient change observed for both phases was ~6500 M^{-1} cm^{-1}, approximately equal to the reduction of one flavin per subunit [38]. Together, these data show slow reversible reduction of the enzyme by NADPH in the absence of pyrimidine substrates.

In the presence of uracil, the initial rate of reduction was approximately two orders of magnitude more rapid, resulting in the conclusion that bound pyrimidine promotes hydride transfer from NADPH and establishing an effector role for the pyrimidine substrate [36,38]. For the enzymatic reaction under anaerobic conditions, it was proposed that the $NADP^+$ formed in the reaction was inhibitory and prevented the complete reduction of the equivalent of one flavin per subunit. In recent studies the reported fractional reduction observed is accounted for by pyrimidine induced two-electron reductive activation of the enzyme prior to catalytic reduction of the pyrimidine (see below) [38].

6. Recent findings that reframe the catalytic mechanism of DPD

The first structures of mammalian DPD settled numerous questions for the chemistry involved [28,29,55]. These data made it plain that two hydride transfer events bookend transmission of two electrons across a

56 Å span via four Fe_4S_4 centers that act as a wire (Fig. 4). This architecture creates mechanistic constraints that require the flavins mediate the two-electron, hydride transfers that occur from and to the NADPH and pyrimidine substrates and the one-electron chemistry that occurs at the Fe_4S_4 centers. Hagen et al., showed that the resting form of DPD is EPR silent and so all Fe_4S_4 centers are assumed to be in the 2^+ state [31,43]. It is therefore surmised that in order to sequentially transmit electrons through the chain of Fe_4S_4 centers during catalytic turnover the FAD and FMN will cycle between oxidized to hydroquinone to semiquinone states. These constraints, however, do not define the order of events that result in pyrimidine reduction and recent data have revealed rather unexpected sequences for electron transfers within DPD, that arise from the requirement for two-electron reductive activation before pyrimidine reduction can occur. In this section we will describe what has recently been deduced from a combination of steady-state and transient-state reactions of wild type and variant DPDs studied under anaerobic conditions [38,39,58]. The experiments described reveal the net chemistry that occurs in each step observed and Fig. 7 summarizes the conclusions that were drawn from these data.

As stated, the residue C671 is the necessary proton donor for pyrimidine reduction. Substituting the cysteine with a serine or alanine has shown a respective slowing or abolishment of DPD activity [36,38,39]. The movement of the loop on which C671 resides (Fig. 6) [26,28,29,39] limits the availability of the thiol proton and would appear to dictate the rate of turnover. Importantly, the C671S variant delineated successive events in single turnover, permitting an account to be made of electrons entering the protein based on spectrophotometric deconvolution and quantitative product analyses that together expanded the understanding of DPD's electron transfer processes [38,39].

6.1. *Reductive activation*

Anaerobic transient-state spectrophotometric analyses of the DPD C671S variant established that when DPD is combined with limiting NADPH and excess pyrimidine, the reaction exhibits two phases when observed at 340 nm [38]. The rate of the first phase was shown to be dependent on the enzyme form (WT or C671S) while the second rate was tied to both the enzyme form and pyrimidine substrate (uracil or thymine) and the amplitude of the second phase was proportional to the concentration of available pyrimidine. The first phase was shown to

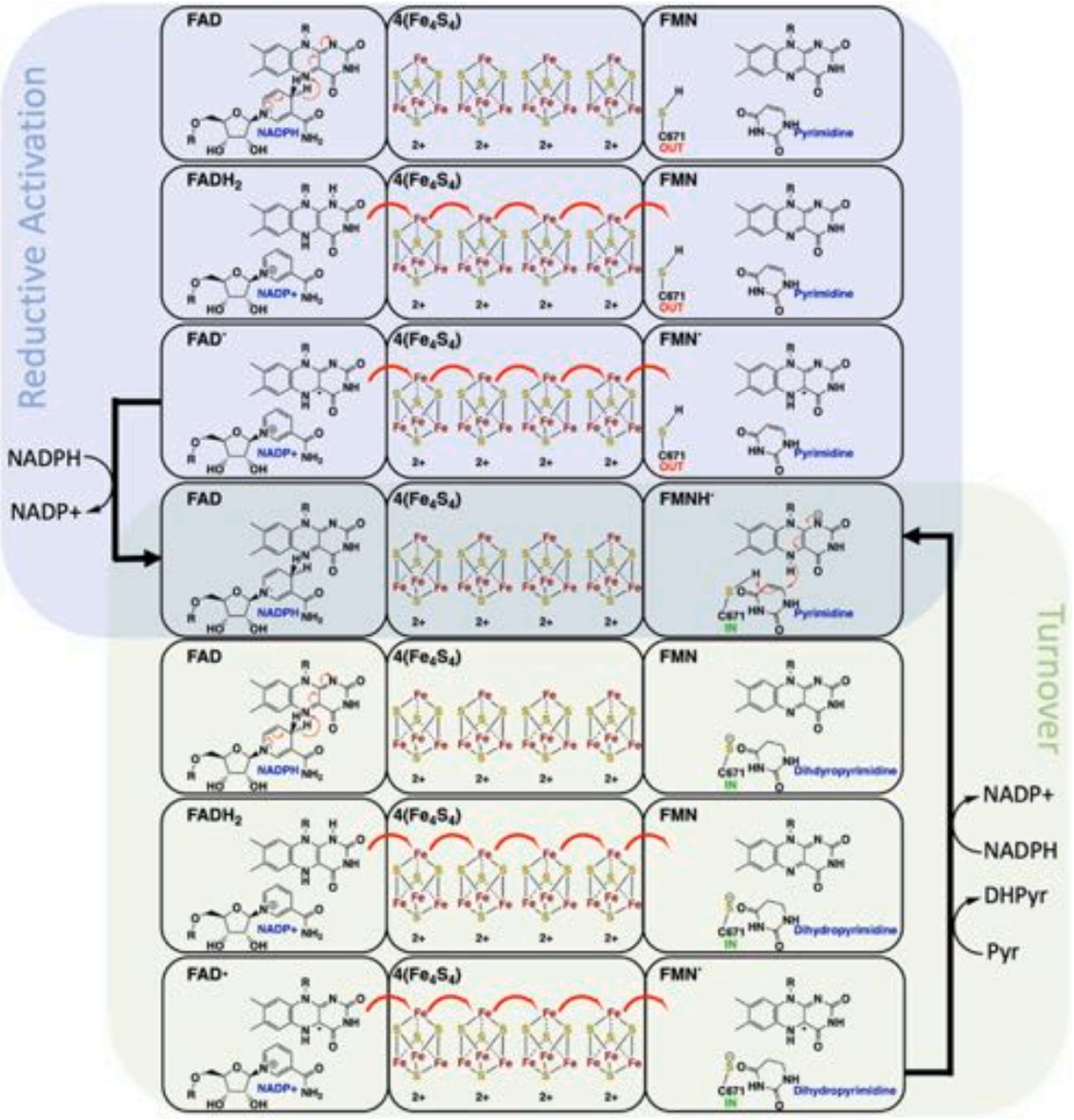

Fig. 7. The proposed steps in reductive activation and turnover of DPD

consist of reduction of a flavin within the enzyme with oxidation of NADPH and that this process was rapid only in the presence of pyrimidine substrate. In this phase NADPH equal to one half the enzyme concentration (as defined by subunit concentration) is oxidized with concomitant reduction of one of the two flavins of one subunit. This apparent half-reaction stoichiometry was surmised to be a result of the reductively activated subunit having high affinity for NADPH and therefore sequestering the residual NADPH, out-competing NADPH binding and activation at the second subunit. This supposition was qualitatively confirmed by simulation of the observed phases using a comprehensive kinetic model in which the dissociation constant for NADPH for the reductively activated subunit was three orders of magnitude smaller than for the non-activated enzyme.

At low pH values the reductive activation phase was delineated further, revealing an additional early phase [39]. This phase was assigned as resulting from the binding of NADPH adjacent to the FAD cofactor. The difference spectrum for this phase indicated that NADPH binding perturbs the DPD spectrum in the visible region and induces broad long-wavelength charge transfer (CT) transitions. In the presence of limiting NADPH the CT transitions decay with the subsequent phase in which the enzyme is reductively activated indicating that the FAD is restored to the oxidized state and implicating the FMN as the recipient of the two electrons that activate the enzyme. Conversely, in the presence of excess NADPH the CT transitions are sustained indicating that the FAD•NADPH complex is reformed by NADP ligand exchange, consistent with the activated enzyme exhibiting high affinity for NADPH. The deconvoluted difference spectra for each of the two early reductive activation phases show only evidence of NADPH binding in the first event followed by flavin reduction and NADPH oxidation in the second, demonstrating that hydride transfer from NADPH to FAD is rate limiting in activation and that electron transmission from $FADH_2$ to FMN is relatively rapid such that $FADH_2$ is not observed to accumulate. This was verified by transient-state kinetic isotope effect (KIE) single-turnover experiments with the C671S variant using excess pyrimidine and limiting NADPH or Pro-S NADPD. The experiment returned a KIE of ~1.9 for the reductive activation phase confirming that the hydride transfer from NADPH to the FAD isoalloxazine is rate limiting for enzyme activation [39]. The reduction of the FMN cofactor during reductive activation was demonstrated directly by soaking NADPH to crystals of the DPD•thymine complex under near anaerobic conditions. The resulting 1.69 Å resolution structure clearly indicated pleating of the FMN cofactor along the N10–N5 axis of the isoalloxazine consistent with the expected sp^3 geometry of reduced flavin [39].

The pH dependence of the observed rate constants for the two phases of reductive activation showed that the rate of binding of NADPH was largely independent of pH and that the reduction of FMN, via the cofactors of the electron transfer conduit, was highly dependent on pH. The reduction of FMN increased in observed rate constant with increasing pH with a pK_a of 7.9 [39]. This pK_a was tentatively assigned to a group on or near the FAD cofactor that when deprotonated enhances electron transfer from NADPH to FAD and on to the FMN. This assignment was in part based on the assumption that electrons rapidly depart the $FADH_2$ state due to the lowering of the reduction potential of the FAD by a clustering of proximal negative charges (Fig. 5). The active state of DPD was thus shown to have the cofactor set of FAD-4 (Fe_4S_4)-$FMNH_2$ and this two-electron reduced state of the enzyme was shown to remain even in the presence of saturating oxidant pyrimidine [38]. The FMN cofactor thus is behaving as an electron sink, receiving electrons from across the assumed low resistance conduit formed by the $FADH_2$ and iron-sulfur centers [39].

Structural data for DPD solved in the presence of substrates under near anaerobic conditions reveal that the mobile loop that carries the FMN active site general acid, C671, moves from an open to a closed state with reductive activation. This conformational change both positions the cysteine thiol adjacent to the pyrimidine substrate and occludes the active site from solvent (Fig. 6). Interestingly, only in the presence of NADPH does pyrimidine reduction take place, indicating that the two active sites have contingent processes that communicate substrate occupancy.

5EU is FDA approved and has been clinically studied as an adjunct chemotherapy sensitizer to enhance the toxicity of 5FU [21,23,60–65]. Though not yet adopted into standard of care protocols, it is established in rodents that 5FU levels are sustained by its co-administration [19]. The *in vitro* interaction of 5EU with DPD has been investigated in two studies and has proven instructive for the mechanism of reductive activation. In the first study, Porter et al. demonstrated reversible binding to the resting enzyme with a K_d of 1.6 μM and showed that irreversible inactivation could be measured only in the presence of NADPH and that it occurred with rate constant of 0.3 s^{-1}. These researchers also identified covalent attachment of 5EU to an active site cysteine residue [25]. More recently Forouzesh et al. studied kinetic and structural aspects of covalent inactivation of DPD by 5EU. In this study the inactivation rate constant was found to be in good agreement with the Porter et al. study (0.2 s^{-1}). It was also shown that NADPH was oxidized during inactivation and via a combination of anaerobic transient state methods and spectral deconvolution it was shown that one flavin is reduced per subunit concomitant with inactivation of the enzyme. This 1:1 NADPH:(flavin/subunit) stoichiometry for reductive activation differs from the 0.5:0.5 ratio observed for reductive activation with native substrates. These data indicate that 5EU is an effector molecule much the same as native pyrimidines that stimulates DPD reductive activation by NADPH and that this chemistry is required for crosslinking to occur. This structural basis for this was also reported. Three X-ray crystal structures were solved that capture the sequence of events in the 5EU inactivation reaction. These structures show that in the absence of NADPH the target cysteine is 10.5 Å from the ethynyl group of 5EU and that binding and oxidation of NADPH brings this cysteine within 3.3 Å promoting crosslinking and indelible inactivation.

6.2. Pyrimidine reduction

The substrate stoichiometries for the transient state phases of the DPD reaction were obtained using single-turnover reactions of C671S DPD with excess pyrimidine and limiting NADPH that were acid quenched and subject to HPLC product analysis [38]. Comparing the formation of $NADP^+$ with the reduction of pyrimidine throughout the reaction determined the ratio of NADPH consumption and pyrimidine reduction to be 2:1. NADPH is oxidized both in the reductive activation phase and in the subsequent phase concomitant with reduction of an equivalent of pyrimidine. This demonstrated that the first phase of DPD single turnover is a reductive activation and the second is pyrimidine reduction [38].

The difference spectrum for the pyrimidine turnover phase of DPD in single turnover with saturating uracil and limiting NADPH showed characteristics of substrate binding around 500 nm added to the absorbance change for oxidation of NADPH at 340 nm [38]. The difference spectra showed NADPH oxidation comparable to the reductive activation phase, indicating pyrimidine reduction occurs with NADPH oxidation and is distinct from the reductive activation process. An additional aspect of the difference spectrum for pyrimidine reduction is the absence of a reciprocal change at ~480 nm when compared to the activation difference spectrum. The lack of an observed flavin oxidation event during pyrimidine reduction even in the presence of excess uracil indicates the enzyme's activated redox state (FAD-4(Fe_4S_4)-$FMNH_2$) persists [38,39]. This therefore suggests the oxidation of NADPH observed in the pyrimidine reduction phase is used to reinstate the $FMNH_2$ *after* electrons are transferred to the pyrimidine [39].

pH profiles for the rate of WT and C671S DPD turnover were undertaken to ascertain if the pK_a of the active site general acid C671 controlled the rate of catalysis. For both forms of DPD the turnover number reports the rate of pyrimidine reduction [38]. This rate was shown to increase ~4-fold from low to high pH, opposite to the trend for

titration of a cysteine thiol. Calculated pK_as were 7.9 and 7.0 for WT and C671S respectively. While the pK_a for the WT could be attributed to the active site cysteine residue, the number for the variant form cannot reasonably be assigned to a serine residue. These data collectively suggest that a different group from the C671 thiol is titrated with pH and that the protonation state influences the rate of pyrimidine reduction. The N1 proton of the $FMNH_2$ was hypothesized as a potential candidate having a pK_a of 6.7 in solution [39]. It was proposed that the observed pK_a's report the protonation state of the $FMNH_2$, attributing the increased rate of pyrimidine reduction to the anionic form of the reduced cofactor that is more prone to delocalize electrons to reduce the pyrimidine [39].

The effect of solvent deuterium for WT DPD was assessed in the presence of excess NADPH and uracil. The proton inventory data were fit best to a solvent kinetic isotope effect (SKIE) of 3.4 that includes significant fractionation factors indicative of the movement of a thiol-derived proton establishing that proton transfer from C671 is occurring in the rate limiting step. The SKIE data could have also been attributed to two exchangeable protons, but the data did not permit definitive discrimination of the two possibilities. Two exchangeable hydrogens are in-flight in the pyrimidine reduction transition state. One as a hydride from the reduced FMN N5 and the second from the thiol of C671. These transfers are inferred to be concerted as the C671A variant can only reductively activate and does not turnover with pyrimidines. As such pyrimidine reduction is dependent on the conformational availability of the C671 and the SKIE value is likely multiplicative for concerted movement of both deuterons.

The indication of rapid transferal of electrons across the protein is based on the absence of observed intervening reduced states of the enzyme during catalysis. With the exception of small perturbations to the flavin spectra from ligand association, no spectrophotometric evidence for the accumulation of a reduced state beyond FAD-4(Fe_4S_4)-$FMNH_2$ has been detected. This has been interpreted as the enzyme operating observationally analogous to a Newton's cradle; two electrons enter the transfer conduit from NADPH as two more exit with the dihydropyrimidine. The actual order of events may undermine the value of this analogy as pyrimidine reduction is likely to be the instigating step in catalysis followed by NADPH oxidation to reinstate the active enzyme [37]. Despite apparent rapid electron transmittance, DPD turnover is relatively slow (0.8 s^{-1}). It has been proposed that mobility of the 669–684 loop, and with it the C671 residue, limits opportunity for concerted hydride-proton transfer; a limitation that governs the overall rate of catalysis [39].

7. Conclusive remarks

DPD has been a curiosity for enzymologists for more than fifty years. The unexpectedly complex cofactor arrangement seems unnecessarily elaborate in that highly similar chemistry is accomplished by numerous smaller single-domain enzymes that carry only a single flavin cofactor. Nonetheless, the linear path formed by the Fe_4S_4 centers to transmit electrons between the NADPH and pyrimidine, each bound in active sites separated by ~60 Å, would appear to define mechanistic possibilities. From inspection of the enzyme's structure one can appropriately deduce that two obligate two-electron reactions bookend multiple obligate one-electron transfers and that these steps are mediated by the oxidoreductive versatility of the flavins that occupy each active site. Recent advances in the study of DPD have shown that the above deductions are likely correct, but also that the functional state of the enzyme is two-electron reduced at the FMN and that this oxidation state directs an unexpected order of events to bring about pyrimidine reduction and reinstatement of the active enzyme. Fig. 7 depicts a hypothetical mechanism that accounts for much of the recent data assembled for DPD. In this figure it is assumed that a primary function of DPD is the reduction of the FMN cofactor via the FAD-4(Fe_4S_4) conduit with electrons from NADPH. The FMN is assumed to have a relative high reduction potential such that electrons cascade in energy from the NADPH/FAD to the FMN. This process is observed as a reductive activation phase when non-activated, oxidized DPD is combined with pyrimidine and NADPH and as a back-filling reaction after the $FMNH_2$ cofactor passes a hydride to the pyrimidine. In such a mechanism, reduction of the pyrimidine is the instigating and rate-limiting step in catalysis. Reductive reactivation then follows and occurs with a rate more rapid than pyrimidine reduction accounting for the fact that no other reduced state of the enzyme is observed in turnover. Pyrimidine reduction occurs slowly as it is contingent on the proximity of the active site cysteine general acid that resides on a mobile loop that is constantly moving between two conformational states that open and close access to the FMN/pyrimidine active site.

In some respects, it is a cyclical argument to define pyrimidine reduction from $FMNH_2$ as the instigating step in the reaction given that the NADPH is oxidized to reduce the FMN cofactor. However, the fact that the FAD-4(Fe_4S_4)-$FMNH_2$ state persists in the presence of excess pyrimidine substrate and the absence of NADPH indicates that the two-electron reduced form is the resting active state of the enzyme. Moreover, for the reductive (re)activation of DPD to occur at a catalytically relevant rate pyrimidine must be bound in the FMN/pyrimidine active site. This requirement specifies that the two active sites can relay ligand complexation information and will only reduce pyrimidine when NADPH is bound. Though it has not been demonstrated what mechanism links the two active sites, one possibility for the FAD-4(Fe_4S_4)-$FMNH_2$ state is that the average position of the 669–684 loop is biased toward the closed state in the presence of NADPH and the pyrimidine substrate. Only in this conformation is C671 positioned for reduction of the pyrimidine. With the transfer of a hydride and proton to the pyrimidine, oxidation of NADPH backfills the reduced state of the FMN cofactor completing the catalytic cycle.

Targeting the active site general acid cysteine for covalent modification using 5-substituted pyrimidines that mimic the native substrates or products is an effective approach for DPD inhibition [25,27]. These molecules act as effectors and induce reductive activation and closure of the active site loop in which the general acid cysteine resides, placing it proximal to the reactive 5-substituent. From a clinical standpoint, the problem of inhibition of DPD has in large part been solved. 5EU provides targeted and complete mechanism-based covalent inhibition of DPD and is well tolerated by patients [66]. Why 5EU inhibition of DPD during 5FU chemotherapy hasn't yet resulted in a clear advantage compared to other adjunct therapies is a question that has been explored extensively by Spector and others [21,23,60,66,67]. It is possible that excessive 5EU dosing in clinical trials undermined efficacy by causing accumulation of uracil that then competes with 5FU for incorporation into ribonucleotides and thereby diminishes toxicity via 5FdUMP (Fig. 1). In a rat model Spector and Cao were able to show complete tumor regression in 88% of rats tested at 1 mg/kg 5EU and that this rate decreased to 25% at 5 mg/kg [67].

Acknowledgements

This research was supported by Loyola University College of Arts and Sciences and National Science Foundation Grants 1904480 to G.R.M.

References

[1] G. Milano, M.C. Etienne, Dihydropyrimidine dehydrogenase (DPD) and clinical pharmacology of 5-fluorouracil (review), Anticancer Res. 14 (6A) (1994) 2295–2297.
[2] R.B. Diasio, T.L. Beavers, J.T. Carpenter, Familial deficiency of dihydropyrimidine dehydrogenase. Biochemical basis for familial pyrimidinemia and severe 5-fluorouracil-induced toxicity, J. Clin. Invest. 81 (1) (1988) 47–51.
[3] C. Heidelberger, N.K. Chaudhuri, P. Danneberg, D. Mooren, L. Griesbach, R. Duschinsky, R.J. Schnitzer, E. Pleven, J. Scheiner, Fluorinated pyrimidines, a new class of tumour-inhibitory compounds, Nature 179 (4561) (1957) 663–666.
[4] R.J. Rutman, A. Cantarow, E. Paschkis, B. Allanoff, Studies on uracil utilization normal and acetaminofluorene-treated rats, Science 117 (3037) (1953) 282–283.

[5] R.T. Reilly, K.W. Barbour, R.B. Dunlap, F.G. Berger, Biphasic binding of 5-fluoro-2'-deoxyuridylate to human thymidylate synthase, Mol. Pharmacol. 48 (1) (1995) 72–79.
[6] N.M. Mhaidat, M. Bouklihacene, R.F. Thorne, 5-Fluorouracil-induced apoptosis in colorectal cancer cells is caspase-9-dependent and mediated by activation of protein kinase C-delta, Oncol Lett 8 (2) (2014) 699–704.
[7] R. Ponce-Cusi, G.M. Calaf, Apoptotic activity of 5-fluorouracil in breast cancer cells transformed by low doses of ionizing alpha-particle radiation, Int. J. Oncol. 48 (2) (2016) 774–782.
[8] D.B. Longley, D.P. Harkin, P.G. Johnston, 5-fluorouracil: mechanisms of action and clinical strategies, Nat. Rev. Cancer 3 (5) (2003) 330–338.
[9] J.S. de Bono, C.J. Twelves, The oral fluorinated pyrimidines, Invest. N. Drugs 19 (1) (2001) 41–59.
[10] C. Heidelberger, Biochemical mechanisms of action of fluorinated pyrimidines, Exp. Cell Res. 24 (SUPPL 9) (1963) 462–471.
[11] R.J. Kent, C. Heidelberger, Fluorinated pyrimidines. XL. The reduction of 5-fluorouridine 5'-diphosphate by ribonucleotide reductase, Mol. Pharmacol. 8 (4) (1972) 465–475.
[12] G.D. Heggie, J.P. Sommadossi, D.S. Cross, W.J. Huster, R.B. Diasio, Clinical pharmacokinetics of 5-fluorouracil and its metabolites in plasma, urine, and bile, Cancer Res. 47 (8) (1987) 2203–2206.
[13] J. Ludwiczak, P. Maj, P. Wilk, T. Fraczyk, T. Ruman, B. Kierdaszuk, A. Jarmula, W. Rode, Phosphorylation of thymidylate synthase affects slow-binding inhibition by 5-fluoro-dUMP and N(4)-hydroxy-dCMP, Mol. Biosyst. 12 (4) (2016) 1333–1341.
[14] M. Moloney, D. Faulkner, E. Link, D. Rischin, B. Solomon, A.M. Lim, J.R. Zalcberg, M. Jefford, M. Michael, Feasibility of 5-fluorouracil pharmacokinetic monitoring using the My-5FU PCM system in a quaternary oncology centre, Cancer Chemother. Pharmacol. 82 (5) (2018) 865–876.
[15] F. Goirand, F. Lemaitre, M. Launay, C. Tron, E. Chatelut, J.C. Boyer, M. Bardou, A. Schmitt, How can we best monitor 5-FU administration to maximize benefit to risk ratio? Expet Opin. Drug Metabol. Toxicol. 14 (12) (2018) 1303–1313.
[16] M. Tuchman, J.S. Stoeckeler, D.T. Kiang, R.F. O'Dea, M.L. Ramnaraine, B. L. Mirkin, Familial pyrimidinemia and pyrimidinuria associated with severe fluorouracil toxicity, N. Engl. J. Med. 313 (4) (1985) 245–249.
[17] B.E. Harris, J.T. Carpenter, R.B. Diasio, Severe 5-fluorouracil toxicity secondary to dihydropyrimidine dehydrogenase deficiency. A potentially more common pharmacogenetic syndrome, Cancer 68 (3) (1991) 499–501.
[18] A.B. van Kuilenburg, J. Haasjes, D.J. Richel, L. Zoetekouw, H. Van Lenthe, R.A. De Abreu, J.G. Maring, P. Vreken, A.H. van Gennip, Clinical implications of dihydropyrimidine dehydrogenase (DPD) deficiency in patients with severe 5-fluorouracil-associated toxicity: identification of new mutations in the DPD gene, Clin. Cancer Res. 6 (12) (2000) 4705–4712.
[19] T. Spector, J.A. Harrington, D.J. Porter, 5-Ethynyluracil, 776C85): inactivation of dihydropyrimidine dehydrogenase in vivo, Biochem. Pharmacol. 46 (12) (1993) 2243–2248.
[20] S.D. Baker, S.P. Khor, A.A. Adjei, M. Doucette, T. Spector, R.C. Donehower, L. B. Grochow, S.E. Sartorius, D.A. Noe, J.A. Hohneker, E.K. Rowinsky, Pharmacokinetic, oral bioavailability, and safety study of fluorouracil in patients treated with 776C85, an inactivator of dihydropyrimidine dehydrogenase, J. Clin. Oncol. 14 (12) (1996) 3085–3096.
[21] S.D. Baker, R.B. Diasio, S. O'Reilly, V.S. Lucas, S.P. Khor, S.E. Sartorius, R. C. Donehower, L.B. Grochow, T. Spector, J.A. Hohneker, E.K. Rowinsky, Phase I and pharmacologic study of oral fluorouracil on a chronic daily schedule in combination with the dihydropyrimidine dehydrogenase inactivator eniluracil, J. Clin. Oncol. 18 (4) (2000) 915–926.
[22] F. Desmoulin, V. Gilard, M. Malet-Martino, R. Martino, Metabolism of capecitabine, an oral fluorouracil prodrug: (19)F NMR studies in animal models and human urine, Drug Metab. Dispos. 30 (11) (2002) 1221–1229.
[23] E. Rivera, J.C. Chang, V. Semiglazov, O. Burdaeva, M.G. Kirby, T. Spector, Eniluracil plus 5-fluorouracil and leucovorin: treatment for metastatic breast cancer patients in whom capecitabine treatment rapidly failed, Clin. Breast Cancer 14 (1) (2014) 26–30.
[24] R.B. Diasio, Oral DPD-inhibitory fluoropyrimidine drugs, Oncology (Williston Park) 14 (10 Suppl 9) (2000) 19–23.
[25] D.J. Porter, W.G. Chestnut, B.M. Merrill, T. Spector, Mechanism-based inactivation of dihydropyrimidine dehydrogenase by 5-ethynyluracil, J. Biol. Chem. 267 (8) (1992) 5236–5242.
[26] D.C. Forouzesh, B.A. Beaupre, A. Butrin, Z. Wawrzak, D. Liu, G.R. Moran, The interaction of porcine dihydropyrimidine dehydrogenase with the chemotherapy sensitizer: 5-ethynyluracil, Biochemistry 60 (14) (2021) 1120–1132.
[27] D.J. Porter, W.G. Chestnut, L.C. Taylor, B.M. Merrill, T. Spector, Inactivation of dihydropyrimidine dehydrogenase by 5-iodouracil, J. Biol. Chem. 266 (30) (1991) 19988–19994.
[28] D. Dobritzsch, G. Schneider, K.D. Schnackerz, Y. Lindqvist, Crystal structure of dihydropyrimidine dehydrogenase, a major determinant of the pharmacokinetics of the anti-cancer drug 5-fluorouracil, EMBO J. 20 (4) (2001) 650–660.
[29] D. Dobritzsch, S. Ricagno, G. Schneider, K.D. Schnackerz, Y. Lindqvist, Crystal structure of the productive ternary complex of dihydropyrimidine dehydrogenase with NADPH and 5-iodouracil. Implications for mechanism of inhibition and electron transfer, J. Biol. Chem. 277 (15) (2002) 13155–13166.
[30] K.D. Schnackerz, D. Dobritzsch, Y. Lindqvist, P.F. Cook, Dihydropyrimidine dehydrogenase: a flavoprotein with four iron-sulfur clusters, Biochim. Biophys. Acta 1701 (1–2) (2004) 61–74.
[31] H. Beinert, R.H. Holm, E. Munck, Iron-sulfur clusters: nature's modular, multipurpose structures, Science 277 (5326) (1997) 653–659.
[32] G.A. Ziegler, C. Vonrhein, I. Hanukoglu, G.E. Schulz, The structure of adrenodoxin reductase of mitochondrial P450 systems: electron transfer for steroid biosynthesis, J. Mol. Biol. 289 (4) (1999) 981–990.
[33] J.J. Muller, A. Lapko, G. Bourenkov, K. Ruckpaul, U. Heinemann, Adrenodoxin reductase-adrenodoxin complex structure suggests electron transfer path in steroid biosynthesis, J. Biol. Chem. 276 (4) (2001) 2786–2789.
[34] M.A. Vanoni, Iron-sulfur flavoenzymes: the added value of making the most ancient redox cofactors and the versatile flavins work together, Open biology 11 (5) (2021) 210010.
[35] E. Lolis, T. Alber, R.C. Davenport, D. Rose, F.C. Hartman, G.A. Petsko, Structure of yeast triosephosphate isomerase at 1.9-A resolution, Biochemistry 29 (28) (1990) 6609–6618.
[36] K. Rosenbaum, K. Jahnke, B. Curti, W.R. Hagen, K.D. Schnackerz, M.A. Vanoni, Porcine recombinant dihydropyrimidine dehydrogenase: comparison of the spectroscopic and catalytic properties of the wild-type and C671A mutant enzymes, Biochemistry 37 (50) (1998) 17598–17609.
[37] B. Lohkamp, N. Voevodskaya, Y. Lindqvist, D. Dobritzsch, Insights into the mechanism of dihydropyrimidine dehydrogenase from site-directed mutagenesis targeting the active site loop and redox cofactor coordination, Biochim. Biophys. Acta 1804 (12) (2010) 2198–2206.
[38] B.A. Beaupre, D.C. Forouzesh, G.R. Moran, Transient-state analysis of porcine dihydropyrimidine dehydrogenase reveals reductive activation by NADPH, Biochemistry 59 (26) (2020) 2419–2431.
[39] B.A. Beaupre, D.C. Forouzesh, A. Butrin, D. Liu, G.R. Moran, Perturbing the movement of hydrogens to delineate and assign events in the reductive activation and turnover of porcine dihydropyrimidine dehydrogenase, Biochemistry 60 (22) (2021) 1764–1775.
[40] P. Rowland, F.S. Nielsen, K.F. Jensen, S. Larsen, The crystal structure of the flavin containing enzyme dihydroorotate dehydrogenase A from Lactococcus lactis, Structure 5 (2) (1997) 239–252.
[41] P. Rowland, O. Björnberg, F.S. Nielsen, K.F. Jensen, S. Larsen, The crystal structure of Lactococcus lactis dihydroorotate dehydrogenase A complexed with the enzyme reaction product throws light on its enzymatic function, Prot.Sci. 7 (1998) 1269–1279.
[42] R.L. Fagan, M.N. Nelson, P.M. Pagano, B.A. Palfey, Mechanism of flavin reduction in class 2 dihydroorotate dehydrogenases, Biochemistry 45 (50) (2006) 14926–14932.
[43] W.R. Hagen, M.A. Vanoni, K. Rosenbaum, K.D. Schnackerz, On the iron-sulfur clusters in the complex redox enzyme dihydropyrimidine dehydrogenase, Eur. J. Biochem. 267 (12) (2000) 3640–3646.
[44] K. Rosenbaum, K. Jahnke, K.D. Schnackerz, P.F. Cook, Secondary tritium and solvent deuterium isotope effects as a probe of the reaction catalyzed by porcine recombinant dihydropyrimidine dehydrogenase, Biochemistry 37 (25) (1998) 9156–9159.
[45] E.F. Pai, G.E. Schulz, The catalytic mechanism of glutathione reductase as derived from x-ray diffraction analyses of reaction intermediates, J. Biol. Chem. 258 (3) (1983) 1752–1757.
[46] Z.H. Lu, R. Zhang, R.B. Diasio, Purification and characterization of dihydropyrimidine dehydrogenase from human liver, J. Biol. Chem. 267 (24) (1992) 17102–17109.
[47] K. Fink, R.B. Henderson, R.M. Fink, -Aminoisobutyric acid in rat urine following administration of pyrimidines, J. Biol. Chem. 197 (1) (1952) 441–452.
[48] R.M. Fink, K. Fink, R.B. Henderson, beta-amino acid formation by tissue slices incubated with pyrimidines, J. Biol. Chem. 201 (1) (1953) 349–355.
[49] M.T. Dorsett, P.A. Morse Jr., G.A. Gentry, Inhibition of rat dihydropyrimidine dehydrogenase by 5-cyanouracil in vitro, Cancer Res. 29 (1) (1969) 79–82.
[50] B. Podschun, G. Wahler, K.D. Schnackerz, Purification and characterization of dihydropyrimidine dehydrogenase from pig liver, Eur. J. Biochem. 185 (1) (1989) 219–224.
[51] B. Podschun, P.F. Cook, K.D. Schnackerz, Kinetic mechanism of dihydropyrimidine dehydrogenase from pig liver, J. Biol. Chem. 265 (22) (1990) 12966–12972.
[52] B. Podschun, Stereochemistry of NADPH oxidation by dihydropyrimidine dehydrogenase from pig liver, Biochem. Biophys. Res. Commun. 182 (2) (1992) 609–616.
[53] B. Podschun, K. Jahnke, K.D. Schnackerz, P.F. Cook, Acid base catalytic mechanism of the dihydropyrimidine dehydrogenase from pH studies, J. Biol. Chem. 268 (5) (1993) 3407–3413.
[54] D.J. Porter, T. Spector, Dihydropyrimidine dehydrogenase. Kinetic mechanism for reduction of uracil by NADPH, J. Biol. Chem. 268 (26) (1993) 19321–19327.
[55] D. Dobritzsch, K. Persson, G. Schneider, Y. Lindqvist, Crystallization and preliminary X-ray study of pig liver dihydropyrimidine dehydrogenase, Acta Crystallogr D Biol Crystallogr 57 (Pt 1) (2001) 153–155.
[56] T. Shiotani, G. Weber, Purification and properties of dihydrothymine dehydrogenase from rat liver, J. Biol. Chem. 256 (1) (1981) 219–224.
[57] K. Rosenbaum, B. Schaffrath, W.R. Hagen, K. Jahnke, F.J. Gonzalez, P.F. Cook, K. D. Schnackerz, Purification, characterization, and kinetics of porcine recombinant dihydropyrimidine dehydrogenase, Protein Expr. Purif. 10 (2) (1997) 185–191.
[58] B.A. Beaupre, J.V. Roman, G.R. Moran, An improved method for the expression and purification of porcine dihydropyrimidine dehydrogenase, Protein Expr. Purif. 171 (2020) 105610.
[59] Q.H. Gibson, B.E.P. Swoboda, V. Massey, Kinetics and mechanism of action of glucose oxidase, J. Biol. Chem. 239 (1964) 3927–3934.
[60] M.T. Paff, D.P. Baccanari, S.T. Davis, S. Cao, R.L. Tansik, Y.M. Rustum, T. Spector, Preclinical development of eniluracil: enhancing the therapeutic index and dosing convenience of 5-fluorouracil, Invest. N. Drugs 18 (4) (2000) 365–371.

[61] S. Cao, D.P. Baccanari, S.S. Joyner, S.T. Davis, Y.M. Rustum, T. Spector, 5-Ethynyluracil, 776C85): effects on the antitumor activity and pharmacokinetics of tegafur, a prodrug of 5-fluorouracil, Cancer Res. 55 (24) (1995) 6227–6230.
[62] R.L. Schilsky, R. Bukowski, H. Burris 3rd, H. Hochster, M. O'Rourke, J.G. Wall, S. Mani, T. Bonny, J. Levin, J. Hohneker, A multicenter phase II study of a five-day regimen of oral 5-fluorouracil plus eniluracil with or without leucovorin in patients with metastatic colorectal cancer, Ann. Oncol. 11 (4) (2000) 415–420.
[63] R.B. Diasio, Can eniluracil improve 5-fluorouracil therapy? Clin. Colorectal Cancer 2 (1) (2002) 53.
[64] D. Yip, C. Karapetis, A.H. Strickland, C. Steer, C. Holford, S. Knight, P. Harper, A dose-escalating study of oral eniluracil/5-fluorouracil plus oxaliplatin in patients with advanced gastrointestinal malignancies, Ann. Oncol. 14 (6) (2003) 864–866.
[65] J.L. Grem, N. Harold, J. Shapiro, D.Q. Bi, M.G. Quinn, S. Zentko, B. Keith, J. M. Hamilton, B.P. Monahan, S. Donavan, F. Grollman, G. Morrison, C.H. Takimoto, Phase I and pharmacokinetic trial of weekly oral fluorouracil given with eniluracil and low-dose leucovorin to patients with solid tumors, J. Clin. Oncol. 18 (23) (2000) 3952–3963.
[66] B.G. Czito, T.J. Hong, D.P. Cohen, D.S. Tyler, C.G. Lee, M.S. Anscher, K.A. Ludwig, H.F. Seigler, C. Mantyh, M.A. Morse, A.C. Lockhart, W.P. Petros, W. Honeycutt, N. L. Spector, P.J. Ertel, S.G. Mangum, H.I. Hurwitz, A Phase I trial of preoperative eniluracil plus 5-fluorouracil and radiation for locally advanced or unresectable adenocarcinoma of the rectum and colon, Int. J. Radiat. Oncol. Biol. Phys. 58 (3) (2004) 779–785.
[67] T. Spector, S. Cao, A possible cause and remedy for the clinical failure of 5-fluorouracil plus eniluracil, Clin. Colorectal Cancer 9 (1) (2010) 52–54.